Benefits of the Future Sea Surface Salinity Measurements From SMOS: Generation and Characteristics of SMOS Geophysical Products

Estelle Obligis, Christine Boone, Gilles Larnicol, Sabine Philipps, Benoît Tranchant, and Pierre-Yves Le Traon

***Abstract*—Soil Moisture and Ocean Salinity (SMOS) level 2 and level 3 products are simulated and characterized over a one-year time period. A simulator is first used to evaluate the sea surface salinity (SSS) error of level 2 SMOS products. An optimal interpolation method is then adapted to map the surface salinity in order to simulate a level 3 SMOS product. The quality of the simulated products is satisfactory. The mean error of the SSS at pixel scale is around 1 psu, and the error on the final gridded product fits the Global Ocean Data Assimilation Experiment requirements (0.2 psu).**

***Index Terms*—Brightness temperatures, microwave radiometry, optimal interpolation, remote sensing, sea surface salinity (SSS), Soil Moisture and Ocean Salinity (SMOS).**

I. Introduction

THE European Space Agency's Soil Moisture and Ocean Salinity (SMOS) satellite, which is scheduled for launch in 2008, will be equipped with the MIRAS instrument, an innovative 2-D synthetic aperture interferometer in L-band [1], [2]. One of the objectives is to retrieve sea surface salinity (SSS) from measured brightness temperatures with a precision of 0.2 psu (practical salinity unit) with averages taken over 200×200 km areas and ten days [as suggested in the requirements of the Global Ocean Data Assimilation Experiment (GODAE)].

The primary objective of this paper is to quantify the benefits of future SSS measurements from SMOS by measuring their impact after the assimilation into an ocean forecasting system. This paper deals with the simulation and characterization of SSS level 2 and level 3 data. The use of these simulated data sets for an impact study in the Mercator Ocean model [3] is presented in [4].

For clarification purposes, we remind that level 2 SMOS products will contain instantaneous SSS at pixel scale (around 40-km resolution), whereas level 3 SMOS products will contain averaged SSS in boxes of 200×200 km and ten days.

Manuscript received March 1, 2007; revised July 17, 2007. This work was supported by the European Space Agency under Contract ESTEC AO/1-4505/03/NL/CB.

E. Obligis, C. Boone, G. Larnicol, and S. Philipps are with the Space Oceanography Division, Collecte Localisation Satellites, 31520 Ramonville Saint-Agne, France.

B. Tranchant is with the Centre Européen de Recherche et de Formation Avancée en Calcul Scientifique, 31057 Toulouse Cedex 01, France.

P.-Y. Le Traon is with the Institut Français de Recherche Pour l'Exploitation de la Mer, 29280 Plouzané, France.

Digital Object Identifier 10.1109/TGRS.2007.914802

This paper is divided into three main steps.

1) We use first an SMOS simulator to estimate and characterize a level 2 SSS error. This study is conducted for year 2001 in the North Atlantic.
2) We simulate, for year 2003, SMOS level 2 products by adding to the SSS from the Mercator Ocean model, an error that is consistent with the characteristics obtained in step 1).
3) Finally, these level 2 products and their associated errors are used to generate and characterize SMOS level 3 products. This gridded product is obtained by using an optimal interpolation technique that takes into account SMOS characteristics (sampling and errors) as well as SSS statistical characteristics (covariance).

In this study, the choice of models and data has been done with special care. Nevertheless, it is a first step in the generation of an SMOS level 3 product; several assumptions have been done, in particular, the assumption of uncorrelated instrumental noise, of a perfect theoretical emissivity model, and of perfect correction of the brightness temperatures from external contaminations. It is obvious that once SMOS flies, it will be necessary to perform an equivalent study with a better characterization of the signal and error covariance models.

This paper is divided into four sections. Section II describes the geophysical data sets we used to simulate an SMOS level 2 product and its error. In Section III, we present the methodology to derive SSS errors and how these error characteristics are used to simulate a realistic level 2 product for year 2003. In Section IV, this level 2 product, and its associated error, is used to generate and characterize an SMOS level 3 product. This section contains, in particular, the description of the optimal interpolation method we used. The last section contains conclusions and perspectives for this paper.

Fig. 1 shows a flowchart with the successive steps and tools (models and data) used to perform this work.

II. Datasets

In this section, we describe the data sets used to build level 2 and 3 products and their associated errors. Each data set is related to a specific step of the processing.

A. *For the Estimation of L2 SSS Errors*

The SSS errors are estimated from the output of an SMOS simulator by looking at the difference between retrieved SSS

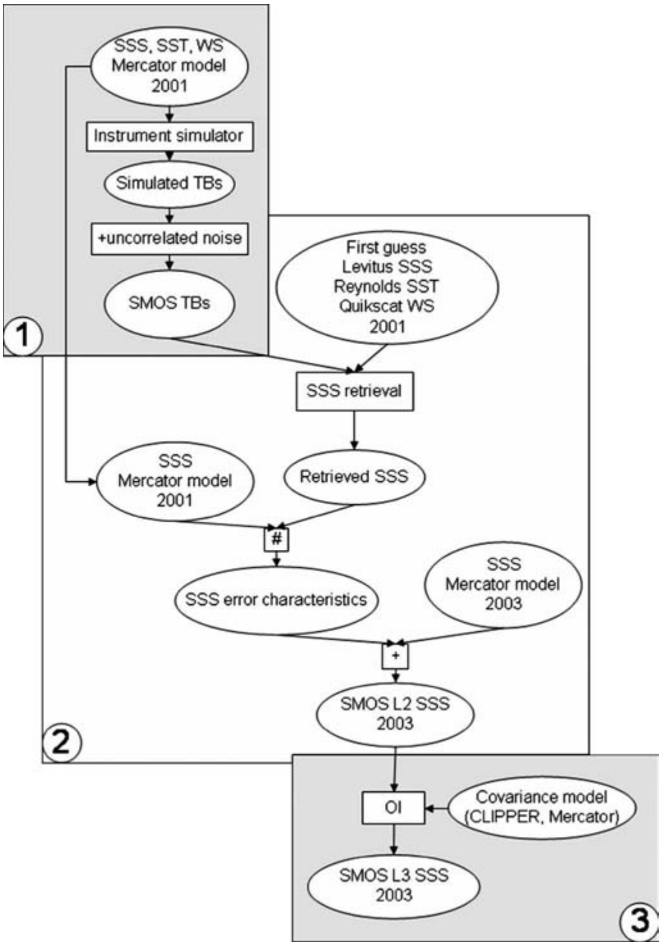

Fig. 1. Flowchart representing the study logic with the different processings, data, and models: Box 1 represents the TB simulations, box 2 represents the generation of SMOS L2 SSS for year 2003, and box 3 represents the generation of SMOS L3 SSS.

and the reference SSS used in input (see Section III-A). Brightness temperatures that are measured in L-band not only depend on SSS but also on sea surface temperature (SST) (because, together with the SSS, it influences the dielectric constant of sea water) and wind speed (WS) (because it provides the information on surface roughness). Therefore, during the SSS retrieval process, first guess values for WS, SST, and SSS are needed. Once SMOS is in flight, these first guess values will be provided by auxiliary data. SST and WS will be extracted from the European Centre for Medium range Weather Forecasts (ECMWF) model, whereas the SSS will be provided by the climatology. To avoid geographically correlated errors, we used independent data sets for the reference and auxiliary values (see [5] for an impact study of potential correlations if this effect is not taken into account).

The reference data sets for SSS and SST are from the Mercator Ocean model PSY1-V1, with the SAM1V1 assimilation system [3], and those for WS are from the ECMWF model. The auxiliary data (used as first guess values) come from Levitus monthly climatology for SSS, Reynolds for SST, and QuikSCAT for WS. ECMWF started assimilating QuikSCAT winds after 2001; thus, the analysis had to be performed no later than 2001. It happens to be the operational start of PSY1-V1,

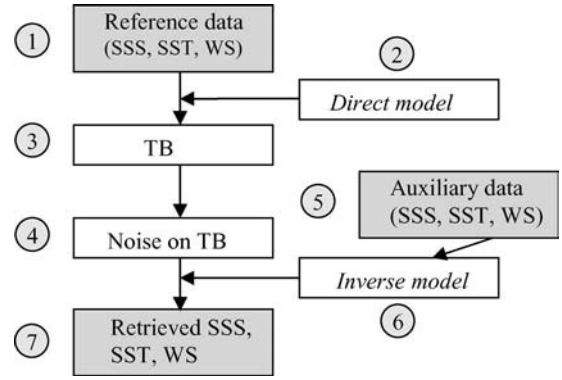

Fig. 2. Functional scheme of the simulator.

which assimilated only sea level anomaly from altimetry (and not SST yet). Thus, year 2001 of PSY1-V1 seemed to be a good candidate for this error study.

These data are used to provide a statistical estimation, leading to the characterization of the SMOS L2 SSS error.

B. For L2 SSS Estimation

One of the goals of this study is the generation of realistic SMOS SSS level 2 and 3 products to be assimilated in the Mercator Ocean model. To have meaningful interpretation of assimilation results, the assimilated SSS should be independent from the one generated by the model itself. Therefore, it was chosen that the SMOS SSS should be estimated from the PSY2-V1 version of the Mercator Ocean model for year 2003 and assimilated in another version (PSY1-V2).

C. For the SSS Time and Space Correlation Estimation

The data set, which is used to estimate the SSS correlation scales needed to parameterize the optimal analysis, is the output of a dedicated CLIPPER model run that did not use any SSS relaxation toward climatology [5]. The available years are 1997 to 1999.

III. Simulation of SMOS L2 Observations: SSS and Its Associated Error

A. Error Characterization

1) SMOS Simulating Tool: A detailed description of the tool we used can be found in [6]. This simulator combines the Ph. Waldteufel simulating tool (see [7]) that takes into account SMOS specificities, and a theoretical orbit provided by Y. Kerr (sun-synchronous with a local solar time of 6:00 A.M. and circular with a repetition of about three days). An illustration of the simplified functionality of the simulator is shown in Fig. 2: TBs (3) are calculated with a direct model (2) from a set of reference geophysical parameters (1), and a noise representing the instrumental and reconstruction error is added to the TBs (4). This noise, which is shown in Fig. 3, depends on both the incidence angle and distance across track and is consistent with other simulation studies [8]. These noisy TBs represent the SMOS measurements and are used to retrieve SSS (7) with an inverse algorithm (6) and a set of auxiliary

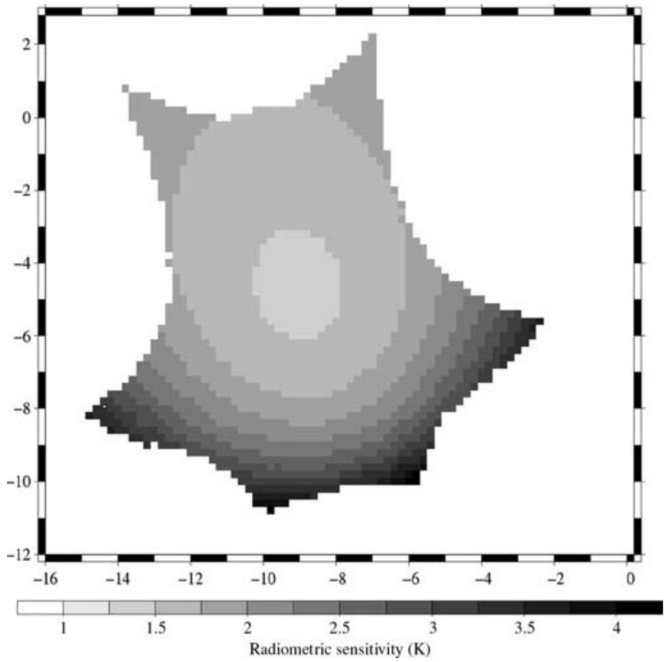

Fig. 3. Radiometric sensitivity within the SMOS field of view. Color scale from 1 to 4 K.

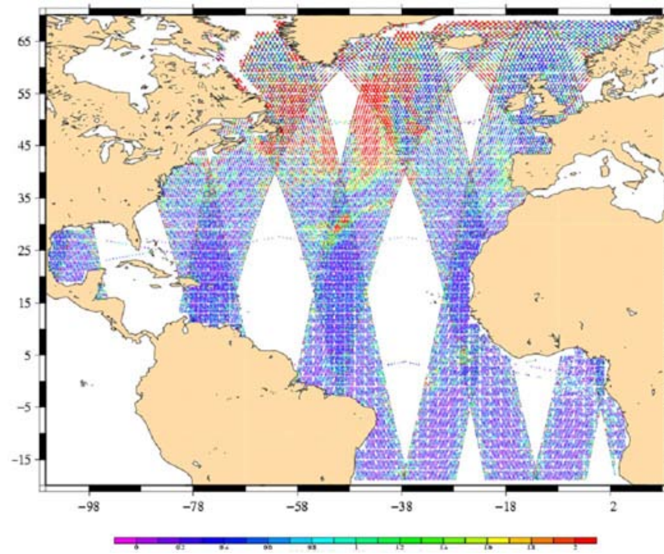

Fig. 4. Error (retrieved–reference SSS) for January 10, 2001–PSY1-V1 area. Color scale from 0 to 2 psu. 4/C

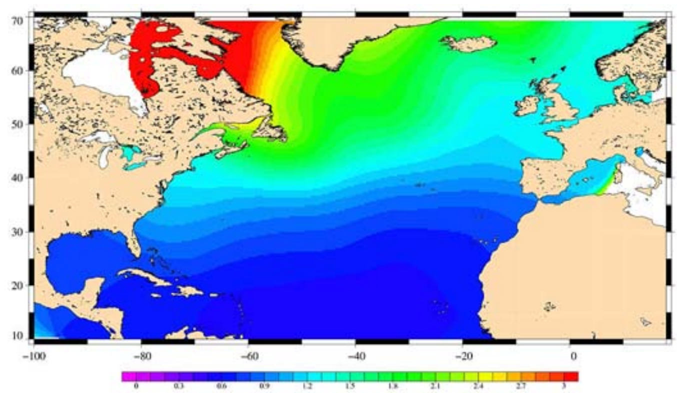

Fig. 5. Estimated level 2 SMOS SSS rms error on monthly bins for January 2001. Color scale from 0 to 3 psu. 4/C

parameters (5). Independent data sets used for reference and auxiliary parameters are described in Section II-A.

Once the measured TBs (4) are simulated (they correspond to the SMOS measurements), an iterative method that is based on the Levenberg–Marquardt algorithm retrieves the SSS. During the inversion, auxiliary data (5) are used as the first guess to compute the TBs which are then compared to the "measured" ones. These first guess values are adjusted to minimize a cost function. This cost function contains the sum of the squared difference between the "measured" and simulated TBs plus the squared difference between the retrieved and auxiliary parameters (SST and WS). All differences are weighted with their respective uncertainties. When the minimum is reached, the modified auxiliary data become the retrieved data. Then, the error is obtained by taking the difference between the reference SSS and this retrieved SSS.

2) Estimation of the Instantaneous SSS Error for Year 2001: The need to estimate a statistical SMOS L2 error is twofold. First, it is used to build an instantaneous error field to create synthetic SMOS L2 SSS, and second, it is the SSS error introduced later in the objective analysis and in the ocean model during assimilation [4]. When SMOS is in flight, validation activities should allow us to estimate a statistical error on the SSS field, which could be used the same way.

The rms of the difference between the retrieved and reference L2 SSSs gives an estimation of the error on the SSS as retrieved from the SMOS measurements. By construction, this error includes the error due to noise on brightness temperatures (box 4 in Fig. 1) that depends on the position of the pixel within the field of view.

The SMOS simulating tool presented in Section III-A-1 is used over one full year (2001) using the data presented in Section II-A. Fig. 4 shows an example of the error (retrieved–reference SSS) map obtained for January 10, 2001. As expected, the error is often lower than 1 psu and increases in high-latitude regions, where the SST is lower, and thus, the sensitivity of the measurement to SSS is weaker.

Then, these instantaneous results are gathered in monthly bins to allow a decent statistical representation of the error. The rms SSS error field found is filtered to conserve only the large-scale structure observed by the future SMOS instrument (see Fig. 5 for the month of January 2001). As previously mentioned, the error is strongly dependent on SST. The case of the January month is extreme for this geographical area, and the errors obtained for the month of July are, for example, much lower (figure not shown).

The smoothing performed allows a more general estimate since we estimate the rms errors from 2001, and we will apply them for the estimation of instantaneous error for 2003. The errors in the Gulf Stream, for example, will not be strongly dependent on a very "accurate" position of the jet, thus allowing for interannual variation of the position of the front.

To estimate the error to add to the SSS daily fields from the Mercator Ocean model PSY2-V1 (that will simulate SMOS SSS for year 2003), the monthly SSS statistical error obtained over 2001 was linearly interpolated every day, and then, a

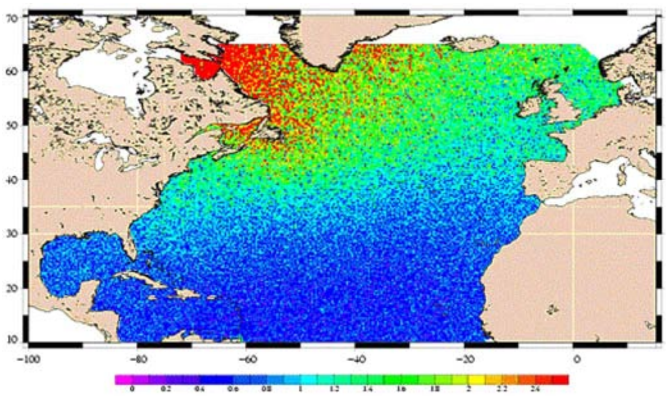

Fig. 6. Reconstructed SMOS L2 SSS error for January 2003. Color scale from 0 to 2.5 psu.

Gaussian noise [called term b in (6)] was generated every day for each point using the local characteristics of the statistical noise (Fig. 6). As an example of the simulation, an instantaneous SSS error at pixel scale is 0.855 psu for January 15, 2001 (using the simulating tool) and is 0.858 psu using our noise reconstruction method for January 15, 2003. Therefore, one can see that the error field is well approximated. One can also see the strong error gradient between warm areas (around the equator) with an increasing error as the temperature cools off toward the northern pole.

B. *Generation of SMOS L2 SSS*

Since the SMOS errors can now be estimated in a fairly trusting fashion, the generation of L2 SMOS SSS is computed from the daily SSS fields from the Mercator Ocean model PSY2-V1 sampled at a 1/3° (roughly the 40 × 40 km from an SMOS mean pixel size) to which we add a Gaussian noise with the characteristics calculated in the previous section. This field is then interpolated on the pixel location for each day. An example of the simulated daily SMOS SSS field for January 15, 2003 is shown in Fig. 7. The top panel represents the SSS field extracted from the Mercator Ocean model, the middle panel represents the error field estimated using the method presented in Section III-A, and the bottom panel represents an L2 SMOS field to be used either in input to generate an L3 product to be directly assimilated in the ocean forecasting system.

IV. Quality Assessment of SMOS Gridded Products (L3)

A. *Method Description*

The L3 SMOS gridded product is defined as a 200 × 200 km × 10 days product with an accuracy requirement of around 0.2 psu. One of the main interests of such a product is a synthesis of the information as well as the reduction of the observation error. This is particularly important in the case of SMOS measurements that exhibit relatively strong errors (around 1 psu with maximum values that can reach 2.5 psu for high-latitude regions). It also presents the advantage to be easy to use for scientific investigation such as the long-term monitoring of the surface salinity variability.

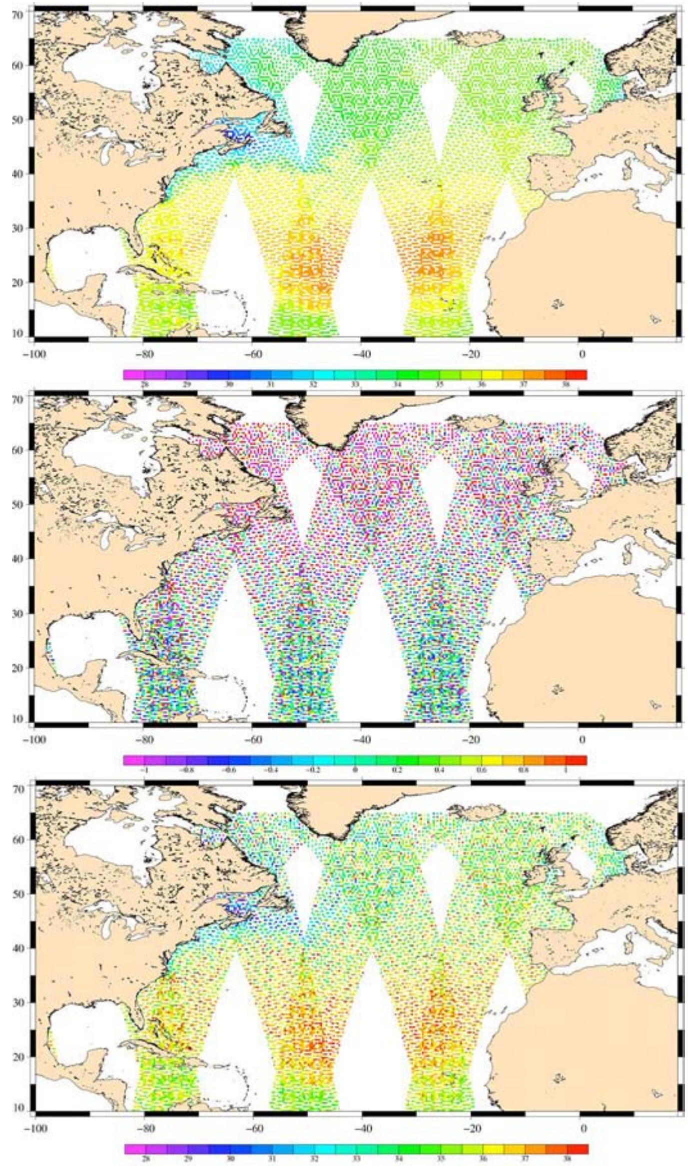

Fig. 7. Steps of the construction of the synthetic SMOS L2 SSS for January 15, 2003. (Top) Mercator model SSS (color scale from 28 to 38 psu), (middle) estimated SSS noise (color scale from -1 to 1 psu), and (bottom) estimated SMOS L2 SSS (color scale from 28 to 38 psu).

The approach chosen to generate the SMOS L3 product is based on optimal interpolation, a methodology firstly introduced in oceanography by Bretherton *et al.* [9] and widely applied to other ocean variables such as sea level altimetry [10], SST [11], or ocean color [12]. The method estimates a value of a field at a given point in space and time from the observations unevenly distributed in space and time. It is based on the *a priori* knowledge of the statistical properties of the field and of the observations covariance errors.

1) Optimal Interpolation Method: In practice, the L3 SMOS SSS value θ_{est} is estimated from the L2 SMOS observations ϕ_{obs} as follows:

$$\theta_{\text{est}}(x) = \sum_{i=1}^{N}\sum_{j=1}^{N} A_{ij}^{-1} C_{xj} \Phi_{\text{obs}^i} \tag{1}$$

where

$\Phi_{\mathrm{obs}^i} = \Phi_i + \varepsilon_i$	the observed measurement, where Φ_i is the true value of SSS, and ε_i is the measurement error;
A_{ij}	the covariance matrix between the observations, as in (2);
C_{xj}	the covariance vector between the observations and the point to be estimated, as in (3).

$$A_{ij} = \langle \Phi_{\mathrm{obs}^i}, \Phi_{\mathrm{obs}^j} \rangle = \langle \Phi_i, \Phi_j \rangle + \langle \varepsilon_i, \varepsilon_j \rangle \tag{2}$$

$$C_{xj} = \langle \theta(x), \Phi_{\mathrm{obs}^j} \rangle = \langle \theta(x), \Phi_j \rangle . \tag{3}$$

The variance of the error associated to the estimation is given by

$$e^2 = C_{xx} - \sum_{i=1}^{N} \sum_{j=1}^{N} C_{xi} C_{xj} A_{ij}^{-1}. \tag{4}$$

The implementation and the configuration of the method are defined by specific parameterizations that are described next.

B. Adaptation and Parameterization of the Method

1) Preprocessing of the Data: The input data of the objective analysis algorithm are expected to be centered. A practical way to center them is to use a "first guess." Different options are possible, starting from the previous analysis, as far as removing a local mean or a climatological field. This problem was already addressed for SST [11] for instance. Both solutions present advantages and drawbacks. However, we choose to use climatology for two reasons. First, it allows us to have consistent statistics for the covariance function calculation, and second, the SMOS mission is not yet launched, and in this case, it seems preferable to use a climatology. The first guess consists in the 2003 yearly mean SSS computed from the Mercator Ocean PSY2-V1 simulations. Then, the L2 SSS observations are used in terms of anomalies with respect to this mean.

Note that the choice of signal covariance functions, as well as errors, should take into account the scales to be resolved in the SMOS level 3 products. For example, if the objective is to map an SSS signal on a $2^\circ \times 2^\circ \times 10$ days grid, the signal covariance function should represent only the large-scale SSS signal, and measurement errors should include subgrid representation errors (i.e., variability smaller than $2^\circ \times 2^\circ$ and 10 days).

2) Variance: The signal variance is deduced from the year 2003 PSY2-V1 runs (Fig. 8) estimated at GODAE scales. Low variability (< 0.05 psu^2) characterized the North Atlantic Ocean. Values greater than 0.5 psu^2 correspond to the Gulf-stream extension and North Atlantic current. At lower boundary of our area, we can distinguish the high tropical variability. Signature of ice melting (0.3 psu^2) is found in high latitudes.

3) Correlation Scales: The estimation of the correlation scales is performed from the CLIPPER free run model ATL6-V7 [5]. This simulated SSS, which is not constrained

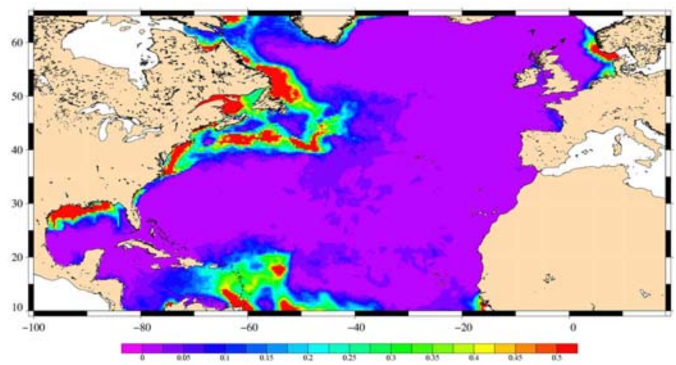

Fig. 8. SSS variance fields deduced from year 2003 of the daily PSY2-V1 Mercator Ocean model simulations. Color scale from 0 to 0.5 psu^2. **4/C**

to climatology, is free to reproduce the natural SSS variability related to the forcing fields (evaporation, precipitation, and runoff) and to the ocean dynamics. Although the atmospheric forcing and the model have known errors, it is expected that the space and time scale variations of SSS are enough realistic to characterize the correlation scales of SSS field.

Time and space correlation scales are calculated on 1/3° grid from three years of data (1997–1999). The observations are selected within a radius of 250 km and 30 days. The empirical correlation function is modeled by using the following classical function:

$$\mathrm{Corr}(x,y,t) = \left(1 + ar + \frac{1}{3}(ar)^2 - \frac{1}{6}(ar)^3\right) e^{-ar} e^{-\left(\frac{t}{Lt}\right)^2} \tag{5}$$

where r is such that $r^2 = x^2/L_x^2 + y^2/L_y^2$, and $a = 3.336912$. L_x and L_y are the space correlation radii mentioned previously, and t and L_t are, respectively, the time and the space correlation radius.

This *a priori* correlation function is then fitted to retrieve the spatial structure of the zonal, meridional, and time correlation scales for SSS.

The zonal [Fig. 9(a)] and meridional scales [Fig. 9(b)] are the highest at the equator and in the tropics (at around 380 and 170 km, respectively) which correspond to the typical equatorial ocean dynamics. The length scales are lower away from the equator due to the mesoscale activity. Some specific areas have large scales, for example, at roughly 32° S–35° W, where zonal length scales reach 450 km above the Rio Grande Rise. The temporal decorrelation scales [Fig. 9(c)] along the equator are low at 10–15 days, which relate well with the equatorial dynamics. It rises at midlatitude from 20 days in region of mesoscale activity (such as the Gulf Stream) up to 40 days in regions of low eddy activity. Large time scales are expected in zones of low variability; however, it is not quite clear why large scales are found in areas such as west of Gibraltar or in the Labrador Sea where the variability is not specifically weak. This could be due to the seasonal cycle.

The derived space and time scales of SSS can be used to define sampling requirements for the observation of SSS mesoscale variability from SMOS. A ten-day time sampling seems appropriate for most of the areas. A $2^\circ \times 2^\circ$ spatial scale

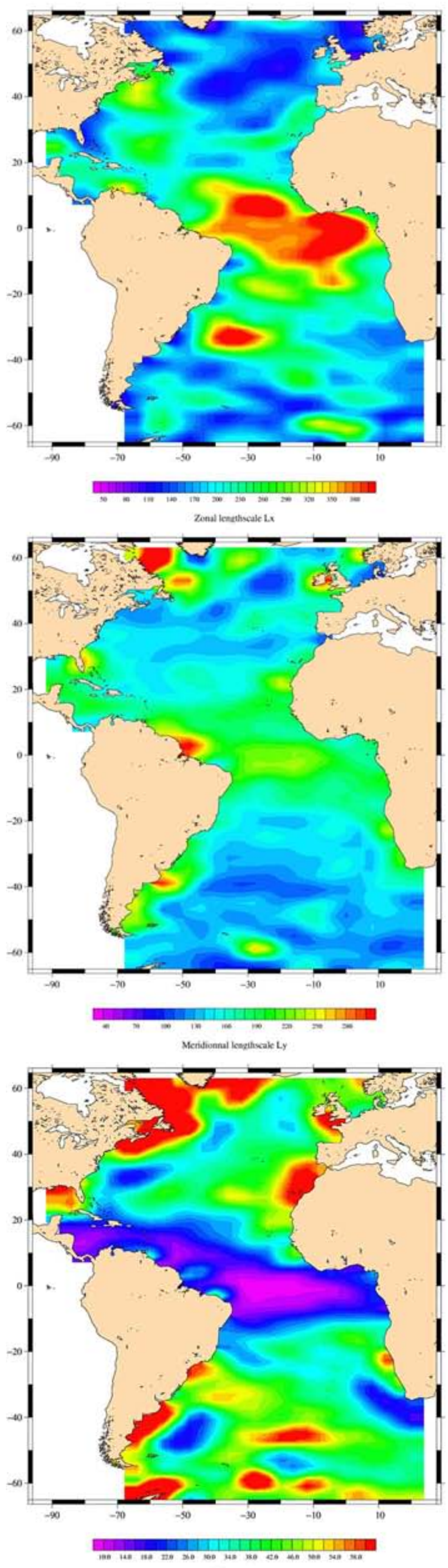

Fig. 9. (a) Zonal (color scale from 50 to 380 km), (b) meridional (color scale from 40 to 280 km), and (c) time (color scale from 10 to 58 days) correlation scales deduced from three years of CLIPPER free run model.

4/C

is, however, adequate only in tropical regions: in mid and high latitudes, a spatial sampling that is better than 100 km is needed to resolve a significant part of the mesoscale variability.

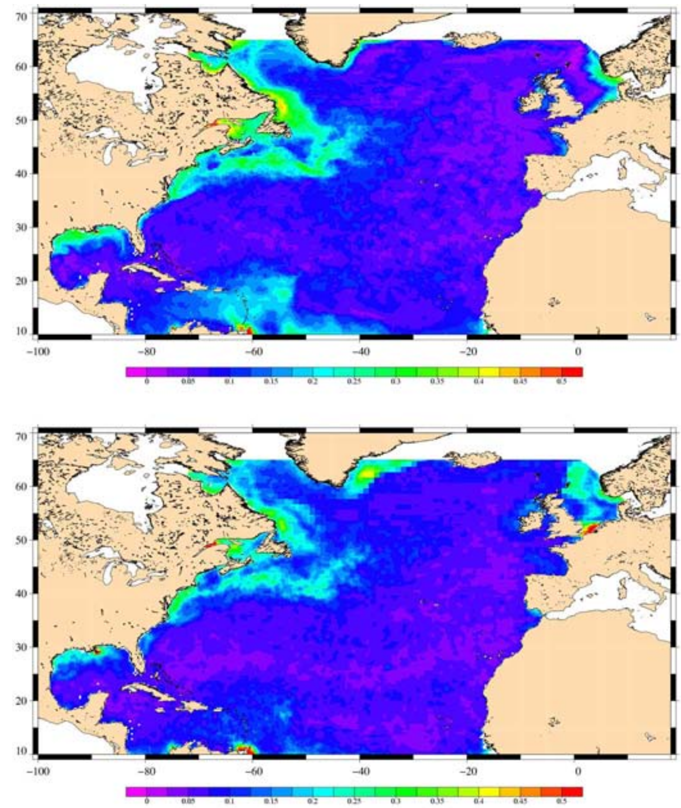

Fig. 10. Top: Annual rms of the SSS mapping error, Bottom: Absolute value of difference between the L3 product (color scale from 0 to 0.5 psu) and reference field (color scale from 0 to 0.5 psu).

4/C

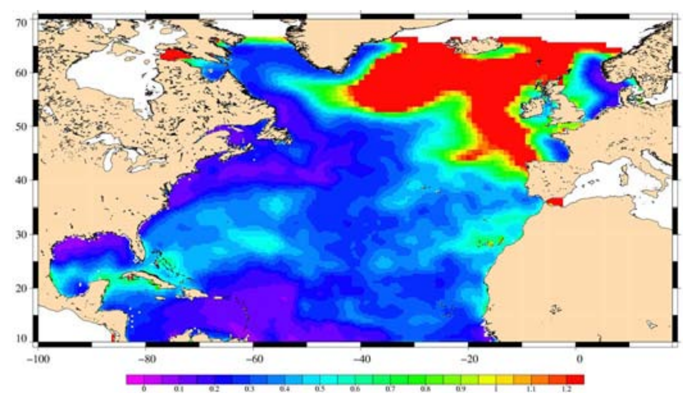

Fig. 11. Mapping error relative to the signal variance observed by Mercator PSY2-V1 (a ratio of 0.6 corresponds to an error of 60% of the signal variance). Color scale from 0 to 1.2.

4/C

Clearly, the scales are varying in space. However, for simplification purposes, we will first look at spatially and temporally constant scales in this paper. We thus choose mean values for the North Atlantic, with a zonal scale of $L_x = 300$ km, meridian scale of $L_y = 200$ km, and temporal scale of $L_t = 10$ days.

4) Observations Error Covariance: The *a priori* error covariance needed for the objective analysis scheme is described in Section III-A2. Due to the important seasonal variability of the measurement noise intensity, we used the monthly estimations. However, it is important to note that this study allows us to estimate only the white noise part of the measurement errors of the future SMOS data. It did not take into account all the different possible sources of error and, in particular, the long wavelength correlated errors that may affect the SMOS level 2 product (galactic noise, correlated errors of the auxiliary data, calibration errors on the brightness temperatures field...). The computation of the error covariance will be calculated as follows:

$$\langle \varepsilon_i, \varepsilon_j \rangle = \delta_{ij} b^2 + E \tag{6}$$

for points i and j, where b^2 is the variance of the white measurement noise (see Section III-A2 for b determination). E is an additional term, not used here, that will allow to take into account the correlated SSS error or the bias between different sensors in order to provide an homogeneous level 4 SSS field, combining SMOS, Aquarius [13], and *in situ* (from ARGO network) observations.

C. *Results and Discussion*

SMOS L3 SSS maps and associated errors are calculated with the methodology described previously. At a 2° regular grid (corresponding to the GODAE product), 51 weekly maps are thus obtained for the whole year 2003.

One way to verify the accuracy of the SSS estimation is to look at the consistency between the formal error deduced from the objective analysis and the differences between the estimated field and the reference field. The annual rms of the SSS mapping error (top) and the absolute value of the difference between the L3 product and the reference field filtered at the GODAE scales (bottom) are shown in Fig. 10. One can note the very good consistency between the two maps both for the amplitude of the error and its spatial structure. Some important differences are situated in high latitudes close to the coast (Greenland and Nordic Sea) where the formal error underestimates the error. This is probably due to local processes, such as ice melting and advection of fresh water from river runoff, that are not well described in our covariance model. In contrary, it seems that the error is overestimated in the western part of the tropics.

On average, the error associated to the L3 product corresponds to the GODAE product accuracy requirement with values that are lower than 0.2 psu almost everywhere, except in the Gulf-Stream area where the error can reach 0.3–0.4 psu. It is important to note that the error of 0.2 psu represents a mean value which does not take into account the local variability of the salinity. Indeed, 0.2 psu could correspond to 10% or 100% of the signal variance. It is shown in Fig. 11 representing the ratio between the mapping error and the signal variance. The error is lower than 40% of the signal variance in the main part of the North Atlantic Ocean, with value smaller than 10% in area of mesoscale variability. On the other hand, highest errors are found in the Northeast Atlantic. This area is characterized, first, by very low variance (< 0.03 psu) and, second, by important error in the SMOS data [Fig. 7(b)] due to the low sensitivity of the SMOS measurement in cold waters. However, the accuracy of the L3 product seems satisfactory in the Labrador Sea despite the large error contained in the L2 SMOS data.

V. Conclusion and Perspectives

In this paper, we described a methodology used to simulate realistic SMOS level 2 and level 3 products that are to be assimilated in the Mercator Ocean forecasting system. We first used an SMOS mission simulator to estimate the SSS error of level 2 SMOS products. An optimal interpolation method was then used to generate and simulate level 3 products.

The quality of the simulated products is satisfactory. The mean error of the level 2 SSS is around 1 psu, and the error of the level 3 SSS fits the GODAE requirements (0.2 psu).

The proposed methodology is used here to simulate SMOS level 3 products. However, the addition of other SSS observations coming from other satellites (e.g., Aquarius) and *in situ* instruments (Argo and thermosalinograph) is already possible, and a similar Observing System Simulation Experiment study with these new data sets should be led in a near future [4].

It would be interesting, in particular, to analyze the consistency and the complementarities between SMOS satellite and Argo array. Indeed, one of the applications of SMOS product concerns the provision of salt fluxes information similarly as the SST does for net heat fluxes. The two observing systems provide a large-scale information of the surface salinity field with specific characteristics: good coverage with relatively high error (both white noise and bias) for SMOS and accurate measurements for Argo but with aliasing of mesoscale signals induced by the sparse sampling of the array. The merging of the two types of observations should allow us to reduce the bias contained in SMOS data and to provide unbiased maps of SSS, which is crucial for modelers.

In this study, geophysical data have been chosen with special care. In particular, we decided to provide the independence between geophysical data used to simulate the TBs and those used as auxiliary parameters in the retrieval process by using two different existing data sets, whereas most of past studies are content with only adding a white noise.

Nevertheless, important error sources have been omitted. The major one is probably the error in the theoretical emissivity model. We used the same theoretical model to simulate and invert the TBs. This implies the assumption that the model is perfect.

The second assumption concerns the instrumental noise. We created a noise with quite realistic variations in the field of view, but assumed uncorrelated values. When SMOS flies, we will probably face with correlated noise (between polarization, from one pixel to the other...). The third assumption concerns the contamination of the brightness temperatures by external sources (sun glint, galactic noise, atmospheric effect, and Faraday rotation). When neglecting entirely these terms in the TBs, we assume that these effects will be perfectly corrected, which is surely not true.

The optimal interpolation provides a formalism to introduce the full covariance errors matrix associated to the observations. Therefore, the main challenge will remain in our capacity to characterize the spectrum of the SMOS measurement errors. In the same time, it will be necessary to improve our representation of the SSS covariance functions by taking into account local processes such as ice melting or advection of fresh water.

ACKNOWLEDGMENT

The authors would like to thank J.-M. Molines and B. Barnier for the CLIPPER model simulations and also N. Reul for the fruitful discussions.

REFERENCES

[1] Y. Kerr, *The SMOS Mission (MIRAS on RAMSES), A Proposal to the Call for Earth Explorer Opportunity Mission*, 1998.

[2] Y. H. Kerr, P. Waldteufel, J.-P. Wigneron, J. Martinuzzi, J. Font, and M. Berger, "Soil moisture retrieval from space: The Soil Moisture and Ocean Salinity (SMOS) mission," *IEEE Trans. Geosci. Remote Sens.*, vol. 39, no. 8, pp. 1729–1735, Aug. 2001.

[3] N. Ferry, E. Rémy, P. Brasseur, and C. Maes, "The Mercator global ocean operational analysis system: Assessment and validation of an 11-year reanalysis," *J. Mar. Syst.*, vol. 65, no. 1–4, pp. 540–560, Mar. 2007.

[4] B. Tranchant, C. E. Testut, L. Renault, N. Ferry, F. Birol, and P. Brasseur, "Expected impact of the future SMOS and Aquarius Ocean surface salinity missions in the Mercator Ocean operational systems: New perspectives to monitor the ocean circulation," *Remote Sens. Environ.*, in press.

[5] A.-M. Treguier, T. Reynaud, T. Pichevin, B. Barnier, J.-M. Molines, A. P. de Miranda, C. Messager, J. O. Beismann, G. Madec, N. Grima, M. Imbard, and C. Le Provost, "The CLIPPER project: High resolution modeling of the Atlantic," *Int. WOCE Newsl.*, vol. 36, pp. 3–5, Sep. 1999.

[6] S. Philipps, C. Boone, and E. Obligis, "The role of averaging for improving sea surface salinity retrieval from the Soil Moisture and Ocean Salinity (SMOS) satellite and impact of auxiliary data," *J. Atmos. Ocean. Technol.*, vol. 24, no. 2, pp. 255–269, Feb. 2007.

[7] P. Waldteufel, J. Boutin, and Y. Kerr, "Selecting an optimal configuration for the Soil Moisture and Ocean Salinity mission," *Radio Sci.*, vol. 38, no. 3, 8051, 2003.

[8] A. Camps, A. Corbella, J. Bara, and F. Torres, "Radiometric sensitivity computation in aperture synthesis interferometric radiometry," *IEEE Trans. Geosci. Remote Sens.*, vol. 36, no. 2, pp. 680–685, Mar. 1998.

[9] F. P. Bretherton, R. E. Davis, and C. B. Fandry, "A technique for objective analysis and design of oceanographic experiments applied to MODE-73," *Deep-Sea Res.*, vol. 23, pp. 559–582, 1976.

[10] P.-Y. Le Traon, F. Nadal, and N. Ducet, "An improved mapping method of multisatellite altimeter data," *J. Atmos. Ocean. Technol.*, vol. 15, no. 2, pp. 522–534, Apr. 1998.

[11] R. W. Reynolds and T. M. Smith, "Improved global sea surface temperature analysis using optimum interpolation," *J. Clim.*, vol. 7, no. 6, pp. 929–949, 1994.

[12] C. Pottier, V. Garçon, G. Larnicol, J. Sudre, P. Schaeffer, and P. Y. Le Traon, "Merging SeaWiFS and MODIS/aqua ocean color data in North and equatorial atlantic using weighted averaging and objective analysis," *IEEE Trans. Geosci. Remote Sens.*, vol. 44, no. 11, pp. 3436–3451, Nov. 2006.

[13] G. Lagerloef, Y. Chao, and F. Colomb, "Aquarius/SAC-D ocean salinity mission science overview," in *Proc. IGARSS*, 2006, pp. 1675–1677.

Estelle Obligis received the Ph.D. degree in physical methods in remote sensing from the Université of Paris 7, Paris Cedex, France, in 1996.

Since 1998, she has been with the Collecte Localisation Satellites, Ramonville Saint-Agne, France, where she is currently in charge of microwave radiometry activity. Her research activity focuses on calibration/validation, retrieval algorithms, and long-term survey for microwave radiometers onboard altimetry missions (Topex, ERS-2, Jason, Envisat). She is also involved in the preparation of the future missions, SMOS, AltiKa, Sentinel 3, and Megha-Tropiques.

Christine Boone received the Engineering diploma from l'Ecole Nationale Supérieure d'Hydraulique et de Mécanique de Grenoble, Grenoble, France and the M.S. degree in physical oceanography from Florida State University, Tallahassee.

For five years, she was with NASA/GSFC, Greenbelt, MD, working on altimeter data analysis. She is currently with the Space Oceanography Division, Collecte Localisation Satellites, Ramonville Saint-Agne, France, working mainly on ocean data analysis and operational oceanography.

Gilles Larnicol received the engineering degree from the Ecole Nationale Supérieure des Techniques Avancées, Paris, France, in 1993 and the Ph.D. degree in the field of ocean data analyses from the University of Bretagne Occidentale, Brest, France, in 1998.

Since 1998, he has been with the Space Oceanography Division, Collecte Localisation Satellites, Ramonville Saint-Agne, France. He has experiences both in operational and research oceanography. He is currently the Head of the Oceanography Department of the Space Oceanography Division.

Sabine Philipps received the M.Sc. degree in meteorology from the University of Leipzig, Leipzig, Germany, in 2002 and the Ph.D. degree in oceanography from the University of Toulouse 3, Toulouse, France, in 2005.

She is currently with the Space Oceanography Division, Collecte Localisation Satellites, Ramonville Saint-Agne, France, working principally on calibration and validation of altimetry data.

Benoît Tranchant received the Ph.D. degree in atmospheric dynamic (sea spray modeling) from Nantes University, France, in 1997.

He has been for the last eight years with the Centre Européen de Recherche et de Formation Avancée en Calcul Scientifique, Toulouse Cedex 01, France, in the French operational ocean forecasting project (Mercator-Océan). The current research theme is data assimilation in operational ocean models.

Pierre-Yves Le Traon received the Ph.D. degree in Physical Oceanography from Toulouse University, in 1990.

He was a Vice-Director of the Space Oceanography Division, Collecte Localisation Satellites, Ramonville Saint-Agne, France. He is currently a Program Director for operational oceanography systems of the Institut Français de Recherche Pour l'Exploitation de la Mer, Plouzané, France. His fields of interest are in operational oceanography, data assimilation, and *in situ* and satellite ocean observing systems. He is a member of the ESA SMOS Science Advisory Group and a Cochair of the Global Ocean Data Assimilation Experiment.